Selected papers presented at the 15th Symposium of Magnetic Measurements and Modelling SMMM'2025

Concept of a Detector for Magnetic Field Distribution in a Measurement System for Nondestructive Testing

J. Salach[a,*] and M. Kiełbiowski[b]

[a] *Warsaw University of Technology, Faculty of Mechatronics, Institute of Metrology and Biomedical Engineering, św. A. Boboli 8, 02-525 Warszawa, Poland*
[b] *Transbit Sp. z o.o., ul. Łukasza Drewny 80, 02-968 Warszawa, Poland*

Doi: 10.12693/APhysPolA.149.S150 *e-mail: jacek.salach@pw.edu.pl

The paper concerns the construction of a system for automatic measurement of the magnetic field distribution on the surface of magnetic materials during their magnetization. Knowledge of this distribution allows one to assess whether a given element has major structural defects, such as cracks, holes, or foreign material inclusions. This is crucial information that determines the suitability of a given element.

topics: magnetic measurement, nondestructive testing, magnetic sensors

1. Introduction

Magnetic nondestructive testing (NDT) enables the detection of critical defects in manufactured parts, such as surface cracks, inclusions, or bubbles, without damaging the tested component [1]. These can be surface or sub-surface defects located up to a depth of approximately 3 mm, depending on the magnetization method and the angle between the direction of the magnetic flux and the defect.

In certain industries, production is carried out exclusively in small batches or single units, which precludes the possibility of sacrificing part of a batch for conventional destructive testing. In such cases, magnetic nondestructive testing can be applied; however, the tested element must be made of a ferromagnetic material [2, 3]. The critical nature of some types of objects, such as components for nuclear power plants, motivates development work in the field of NDT. An equally important industry where this type of testing is essential is biomedical engineering, where every component must undergo rigorous inspection, regardless of production volume.

The magnetic NDT method relies on magnetizing the object under test. If surface discontinuities exist in the material, the magnetic field will leak (scatter) across the object's surface. While narrow defects situated perpendicular to the direction of the magnetic field flow are easily detected, those that are parallel or at a slight angle are either not detected or their detectability is very low. This occurs despite small leakages in the field and is due to the insufficient sensitivity of common methods — most often metal powders accumulating around the field leakage or uniaxial magnetic field sensors. The objective of the measurement is to detect such scattering and determine its location. Based on the magnetic flux leakage map, conclusions are drawn regarding the quality of the tested part without destroying it, allowing it to return to the technological process.

Magnetic nondestructive testing (NDT) methods based on magnetic flux leakage (MFL) are widely used to inspect safety-critical ferromagnetic components in power engineering, transportation, and manufacturing industries. Classical MFL systems employ magnetizing yokes or permanent magnets and detect local perturbations of the magnetic field above the component surface using single-axis sensors or magnetic particles. Although these techniques are well-established in industrial practice, their performance strongly depends on the orientation of the defect relative to the magnetizing field and on the geometry of the sensing arrangement. In particular, defects oriented nearly parallel to the direction of magnetization often generate relatively weak leakage fields, which leads to reduced detectability and increased risk of missed material discontinuities [4].

Recent developments in magnetic NDT include the use of advanced magnetic sensors (Hall effect sensors, magneto-resistive sensors, and fluxgate sensors) and multi-channel probes for detailed mapping of the magnetic field distribution. These solutions enable more precise quantification of the leakage

field and open up the possibility of reconstructing the spatial characteristics of defects. However, many reported systems still rely on one-dimensional measurements of the field amplitude along a scan line and do not provide full information about the vector nature of the magnetic field, which limits the interpretation of signals for complex defect shapes and orientations [5].

In this context, the system presented in this work is designed to provide detailed spatial information about the magnetic field distribution above reference samples with artificial defects. The developed probe uses three Hall effect sensors arranged at 120° to each other, which enables quasi-isotropic acquisition of the magnetic field components in the vicinity of the defect region.

2. Measurement methodology

The aim of the measurement methodology described in this chapter is to determine the spatial distribution of the magnetic field above the tested element and to assess the detectability of surface-breaking defects using a Hall effect probe. The applied method is based on the detection of magnetic field components in the vicinity of artificial defects introduced into ferromagnetic reference samples prepared specifically for probe calibration.

The probe was built as a modular system, with the following indivisible functional units: probe module, 3 × signal amplifier–filter module, microcontroller module, and PC module. The probe module consists of three Hall effect sensors [6] with measurement axes rotated every 120° to best cover the measurement field, as shown in Fig. 1. The amplifier–filter module serves for signal conditioning and interference elimination, whereas the microcontroller and PC modules are responsible for signal processing and data acquisition. The probe enables measurement of the magnetic field strength above the tested element and the direction of the field lines; based on these parameters, the size and orientation of the defect can be estimated. The measured values are reduced to a vector lying in the measurement plane and are determined from the geometric position of the sensors in the probe.

The measurements were performed on reference samples prepared specifically for probe calibration. The samples were made of S235JR steel with good magnetic properties, i.e., permeability of 500, coercivity field of ≈ 100 A/m, and saturation induction $\approx$ 1 T. This is a typical structural steel. The test elements were manufactured to allow for the examination of the probe sensitivity as a function of defect depth and of the angle between the direction of the magnetizing field and the defect length. In the first test element (sample I), a series of incisions was made to imitate defects with depths from 0.1 to 1 mm and a width of 0.4 mm, as shown in Fig. 2. The magnetizing field was directed at an angle of 90° to the length of the incisions. In the second test element (sample II), incisions of the same width and a depth of 0.5 mm were made at angles of 30° and 60° with respect to the magnetizing field direction, as shown in Fig. 3.

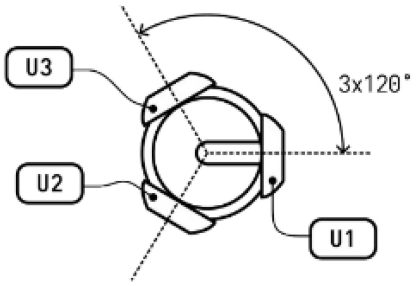

Fig. 1. Diagram of sensor placement in the probe; U1–U3 are Hall effect sensors.

During the measurements, the probe moved along the longitudinal axis of the sample, sequentially approaching predefined measurement points located in the vicinity of the artificial defects. At each position, the components of the magnetic field were recorded and subsequently converted to the magnitude and direction of the resultant field vector in a coordinate system fixed to the probe body. The acquired data were then used to construct field distribution maps above the sample surface and to evaluate the influence of defect depth and orientation on the probe response.

The samples were magnetized using an electromagnetic yoke. The magnetizing field applied to the samples was a static direct current (DC) field. Under these conditions, the probe operated in a quasi-static regime, enabling the measurement of the steady-state distribution of the magnetic field above the defects without additional dynamic effects related to alternating magnetization. The yoke was activated by a push-button switch connected to an external DC power supply, enabling repeatable magnetization conditions during sequential measurement series.

The tests were conducted for a magnetizing field in the tested samples of ≈ 300 A/m. Accurate determination was quite difficult due to a slight shift of the sample relative to the magnetizing device.

3. Results of the investigation

The first series of measurements was carried out on a reference plate with inclined artificial notches of different depths, ranging from 0.1 to 1 mm, and a constant width of 0.4 mm (sample I). The probe was moved along the measurement line above the defect region, and for each predefined point, the amplitude and angle of the reconstructed magnetic field

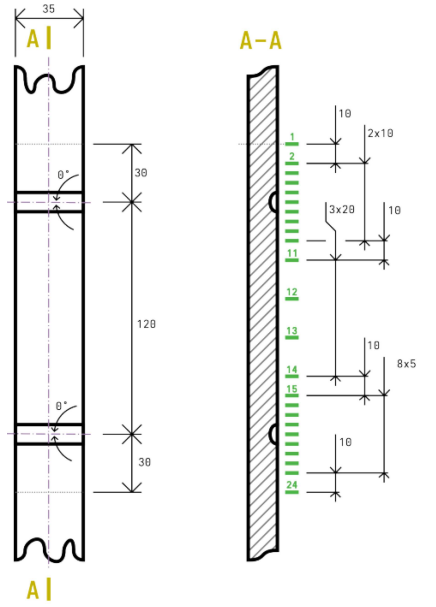

Fig. 2. Reference sample I with 5 imitated defects.

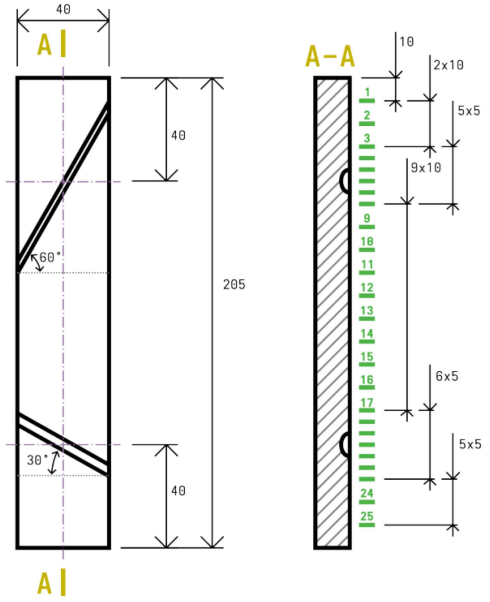

Fig. 3. Reference sample II with imitated defects at angles of 30° and 60°.

vector were recorded. The measured amplitude values and angles of the magnetic field as a function of the physical position along the sample are presented in Fig. 4.

Figure 4 shows that the presence of inclined defects causes a moderate increase in the field amplitude with respect to the background level, while the angular trajectory of the field vector exhibits some fluctuations during measurement. The amplitude increases from values close to the background (approximately a few tenths of the reference unit) up to clearly higher levels in the vicinity of deeper

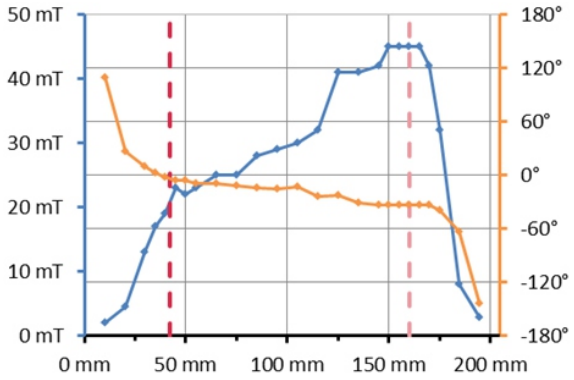

Fig. 4. The values of the magnetic field amplitudes (left) and angles (right) as a function of the position of reference sample II along the measurement line. Blue line — magnetic field amplitude; orange line — angle of the measured magnetic field; red dotted line — angle of 60°; pink dotted line — angle of 30°.

notches, which confirms that the probe is sensitive to changes in defect depth even for nonoptimal angular orientation of the defects. However, the contrast between defective and defect-free regions is lower than in the case of transverse defects, which is consistent with the physics of magnetic leakage field testing for defects oriented at small angles to the magnetizing field. This is because when a magnetic field encounters an obstacle that is not perpendicular, it has an easier path and the field leakage is not as noticeable, and at an angle of 45°, it decreases to almost zero.

The second series of measurements was performed on the reference plate with transverse notches of fixed depth 0.5 mm and width 0.4 mm, oriented at 90° with respect to the magnetizing field in sample II. For this specimen, ten measurement series were acquired along the measurement line, with alternating scan directions (see Fig. 5). For each measurement point, the minimum, maximum, and mean amplitude and standard deviation σ_X (Fig. 6) were calculated, as well as the coefficient of variation V_σ of the magnetic field amplitude (Fig. 7). The standard deviation is described by

$$\sigma_X = \sqrt{\frac{1}{1-n} \sum_{i=1}^{n} \left(x_i - \bar{X}\right)^2}, \tag{1}$$

and the coefficient of variation V_σ is described by

$$V_\sigma = \left(\frac{\sigma_X}{\bar{X}}\right) \times 100\%. \tag{2}$$

The amplitude value graph in Fig. 5 shows pronounced peaks of the magnetic field amplitude at positions corresponding to the locations of the transverse defects, reaching values several times higher than the background level. At the same time, the coefficients of variation in the peak regions remain relatively low, which indicates good repeatability of the probe response in the presence

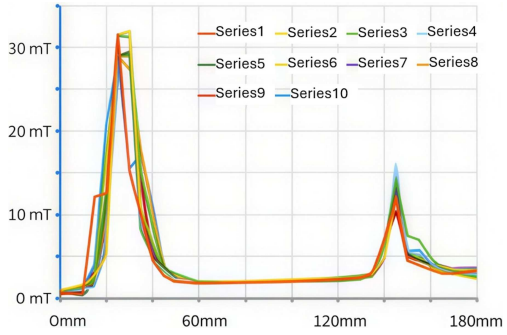

Fig. 5. The amplitude values of the magnetic field as a function of position along the reference sample I.

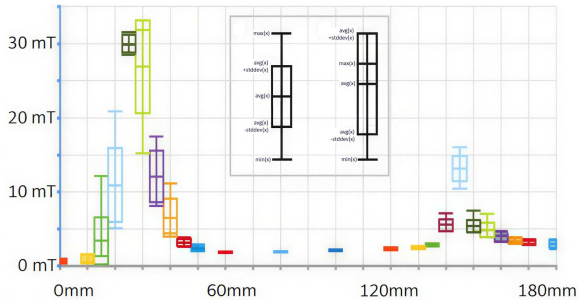

Fig. 6. Sensor characteristics of the minimum, maximum, and mean amplitude and standard deviation.

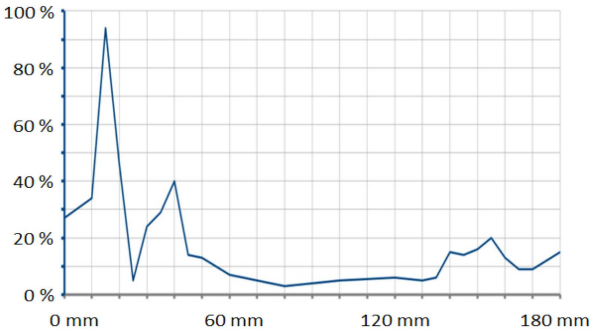

Fig. 7. Coefficient of variation of the magnetic field amplitude.

of defects. This behavior confirms that defects oriented approximately perpendicular to the magnetizing field produce a strong and robust leakage field signal that can be reliably detected by the probe.

To quantify the detectability of defects, a relative response index s_i was introduced, defined as the relative change in the field amplitude between the response peak and the preceding baseline point along the scan, normalized to the baseline amplitude. For each defect and each measurement series, this index was evaluated using the amplitudes in the "point before response" and "peak point" positions identified in the scan. A defect was classified as "detectable" when the index exceeded 100%, whereas responses below this threshold were considered nondetectable. The relative response index s_i is described by

$$s_i = \left| \left(\frac{V_{ti} - V_{bi}}{V_{bi}} \right) \times 100\% \right|, \tag{3}$$

where:

- V_{ti} [V] — probe reading at the peak of the defect reading;
- V_{bi} [V] — probe reading in the area without defects.

The indicator of the significance of the response to the defect can also be described in unitless form as

$$s_i = \frac{V_{ti}}{V_{bi}}. \tag{4}$$

The detailed results of this analysis are summarized in Table I. The term "difference in measurements" refers to the increase in the probe reading above the defect. "Direction of measurement" indicates the direction of probe movement along the sample for a specific measurement result; this designation was introduced due to different field values on the sample surface. These fluctuations are related to the heterogeneity of the plate structure. The direction of probe movement is parallel to the sample plane. In this type of examination, it is important to detect magnetic pool leakage. Its specific value only indicates the size of the defect, not its nature. For the plate with transverse defects, the relative response index significantly exceeds the 100% threshold in all analyzed cases, often reaching several hundred percent, which confirms unambiguous detectability of these defects by the probe. In contrast, for inclined defects, the relative response is lower, which reflects the known limitation of magnetic leakage field methods for defects oriented nearly parallel to the magnetizing field.

4. Conclusions

The experimental results demonstrate that the developed probe fulfills its intended function in magnetic nondestructive testing based on the leakage field method. It provides a clear and statistically significant response to transverse surface-breaking defects of 0.4 mm width and 0.5 mm depth, with good repeatability across multiple measurement series. For inclined defects of the same width and varying depth, the probe remains sensitive to changes in defect depth, but the response contrast is reduced, in agreement with theoretical expectations for defect orientation effects in magnetic testing. The device works correctly for basic defects; further tests are planned for a greater variety of defects in terms of both depth and width. The effect of the angle of position relative to the defect has been verified, but the sensitivity of the instrument for different angles will also be determined.

TABLE I

Detailed results of this analysis.

Measurement series number	Direction of measurement	Defect number	Difference in measurements T	Relative response index s_i	Defect detectability
sample II					
1	↑	1	0.04	1.2	undetectable
		2	0.13	1.4	undetectable
sample I					
1	↓	1	2.9	12.2	detectable
		2	0.85	3.5	detectable
2	↑	1	2.91	11.4	detectable
		2	0.95	4.8	detectable
3	↓	1	2.93	15.7	detectable
		2	1.1	4.5	detectable
4	↑	1	3.01	22.5	detectable
		2	1.29	5.2	detectable
5	↓	1	2.72	12.8	detectable
		2	1.01	3.2	detectable
6	↑	1	2.65	12.0	detectable
		2	1.27	6.5	detectable
7	↓	1	2.7	13.9	detectable
		2	0.97	3.6	detectable
8	↑	1	2.65	12.5	detectable
		2	0.99	4.8	detectable
9	↓	1	2.68	13.8	detectable
		2	0.67	2.8	detectable
10	↑	1	2.48	7.2	detectable
		2	0.87	4.0	detectable

References

[1] A. Bienkowski, R. Szewczyk, J. Salach, *Acta Phys. Pol. A* **118**, 1008 (2010).

[2] M. Kachniarz, J. Salach, *Measurement* **168**, 108301 (2021).

[3] A. Bienkowski, R. Szewczyk, J. Salach, R. Kolano, *Solid State Phenomena* **154**, 23 (2009).

[4] B. Feng, J. Wu, H. Tu, J. Tang, Y. Kang, *Materials* **15**, 7362 (2022).

[5] K. Kosmas, C. Sargentis, D. Tsamakis, E. Hristoforou, *J. Mater. Process. Technol.* **359**, 161 (2005).

[6] A. Wozniak, M, Kretkowski, R, Jablonski, *Metrol. Meas. Syst.* **14**, 351 (2007).